

Response surface modeling and optimization to study the influence of deposition parameters on the electrodeposition of Cu–Zn alloys in citrate medium

F. B. A. Ferreira · F. L. G. Silva · A. S. Luna ·
D. C. B. Lago · L. F. Senna

Received: 10 April 2006 / Accepted: 10 November 2006 / Published online: 5 January 2007
© Springer Science+Business Media B.V. 2006

Abstract Copper–zinc alloy coatings were deposited on mild steel substrates using sodium citrate electrolytes at room temperature and under direct current. For the bath composition studied, factorial design was used to verify the influence of deposition parameters, such as current density and mechanical stirring, on the cathodic efficiency, the contents of copper and zinc, and the amount of hydrogen evolution. Moreover, the four responses were simultaneously studied by using an optimization methodology. The results suggest that the optimum point for reaching good quality copper–zinc alloy deposits from the proposed citrate electrolytes are 29 A m⁻² and 247 rpm for bath 3 and 13 A m⁻² and 67 rpm for bath 4. Applying these conditions, a yellow-reddish coating was obtained from bath 3, while a bright red deposit was produced from bath 4.

Keywords Alloy electrodeposition · Citrate electrolytes · Copper–zinc alloys · Desirability function · Response surface methodology

1 Introduction

The electrodeposition of metal alloys coatings requires the simultaneous reduction of all the metal ions that are forming the alloy at the electrode surface [1, 2]. Therefore, high quality metallic alloy coatings are

usually obtained by using complexing agents, which decrease the activity of the nobler ion in the solution [3]. Cyanide baths have been efficiently used for Cu–Zn alloy coating production, despite their high toxicity and the rigorous maintenance control [4, 5]. Searching for alternative electrolytes to the traditional cyanide ones, several proposed bath compositions have been presented [3, 6, 7]. Some of these are based on citrate for copper [8–10] or zinc [11], and for Cu–Zn [12] alloy electrodeposition. However, even for baths containing only one of the metal ions neither the chelation mechanism nor the electroplating process have yet been clarified, these being dependent on several parameters such as the stability of the metal ion/citrate complex, the citrate concentration and the medium pH [8–10].

The plating of Cu–Zn alloys from citrate bath has not been extensively studied, probably due to the low stability of the baths [12, 13]. Moreover, metal alloy coating electrodeposition is a complex process involving the control of several chemical and operational parameters. In practice, these parameters are often chosen empirically and the alloy is then produced at these “optimum conditions”. Therefore, to improve deposition conditions and produce layers that better fulfill industrial needs, it is important to develop a more scientific approach leading to a clearer fundamental understanding of the co-deposition phenomenon. This will lead to improved process performance and reliability, as well as to the establishment of new alloy systems.

In this work Cu–Zn alloy coatings were produced on mild steel substrates from citrate electrolytes. Using experimental design procedures, the deposition parameters, including current density and mechanical stirring speed, were evaluated for their effects on the

F. B. A. Ferreira · F. L. G. Silva · A. S. Luna ·
D. C. B. Lago · L. F. Senna (✉)
Departamento de Química Analítica, Instituto de Química,
Universidade do Estado do Rio de Janeiro, Rua São
Francisco Xavier, 524, Maracana 20559-900 RJ, Brazil
e-mail: lsenna@uerj.br

cathodic current efficiency, alloy coating composition and hydrogen evolution. The aim of this study was to contribute further insights into the behavior and trends of Cu–Zn electrodeposition from citrate electrolytes in order to attain a more efficient control of the coating properties.

2 Experimental methodology

2.1 Cathodic polarization curves

Cathodic polarization curves were galvanostatically obtained in the current density range of $0.13\text{--}267\text{ A m}^{-2}$. AISI 1028 mild steel discs (exposed area of $1.70 \times 10^{-4}\text{ m}^2$) were used as working electrodes, while a $1.60 \times 10^{-3}\text{ m}^2$ brass plate (63% m/m Cu, 37% m/m Zn) acted as a counter electrode. The reference electrode was a saturated mercury (I) sulfate electrode ($\text{Hg}/\text{Hg}_2\text{SO}_4$), SSE. The experiments were carried out at room temperature and the stirring speed ranged from 0 rpm to 400 rpm. Table 1 describes the chemical composition, pH and conductivity values of the baths.

2.2 Alloy electrodeposition experiments

In order to improve the alloy electrodeposition process and attain a coating composition around 70–80% m/m Cu and 20–30% m/m Zn (commercial brass), an experimental central composite design 2^2 with a central point was employed [14]. A quadratic model was applied to quantitatively evaluate and describe the response surfaces concerning the effects of current density (I) and mechanical stirring speed (S) on the cathodic current efficiency (CCE), the alloy chemical composition (Cu and Zn) and the hydrogen partial current density (I_H) (Table 2). These assays were performed using the same reference and counter electrodes mentioned earlier and mild steel disks with $5.31 \times 10^{-4}\text{ m}^2$ of exposed area as the working electrode. The CCE data were obtained gravimetrically.

Table 1 Chemical composition, pH and conductivity values of the citrate-based electrolytes

Solution	Chemical composition/ mol L ⁻¹			pH	Conductivity/ mS cm ⁻¹
	CuSO ₄	ZnSO ₄	Na ₃ C ₃ H ₆ O ₇		
1	0.02	0.20	0.05	4.08	21.1
2	0.02	0.20	0.10	4.41	23.8
3	0.02	0.20	0.50	5.81	48.7
4	0.02	0.20	1.00	6.30	56.1

Table 2 Central composite design 2^2 experimental matrix

Run no.	Stirring speed	Current density
1	-1	-1
2	+1	-1
3	-1	+1
4	+1	+1
5	0	0
6	0	0
7	0	0
8	$-\sqrt{2}$	0
9	0	$\sqrt{2}$
10	$\sqrt{2}$	0
11	0	$-\sqrt{2}$

The layers produced were dissolved in 20% v/v HNO₃ and the alloy composition was determined by flame atomic absorption spectrometry (FAAS). Table 3 presents the codified and normal values of the studied variables. A commercial software package (STATISTICA for Windows, release 7.0) was used for the experimental data regression analysis.

2.3 Optimization of alloy electrodeposition

The four responses obtained in the electrodeposition experiments (CCE , Cu and Zn contents in the alloy, and I_H) were used to optimize the alloy production using the simultaneous optimization methodology proposed by Derringer and Suich [15]. This is based on the definition of a desirability function for each response, whose values are restricted to an interval of (0,1). The global desirability is then obtained by the geometric average of the individual desirability.

2.4 Corrosion experiments

The coatings obtained in solution 3 (Table 1), at the optimum conditions determined by the optimization of the deposition parameters (I and S), were electrochemically evaluated by anodic potentiostatic polarization curves. The experiments were performed at room temperature in a 0.5 mol L^{-1} NaCl solution. The counter electrode was a platinum spiral, while the reference electrode was saturated calomel (SCE).

Table 3 Codified and normal values of the studied variables

Level	Current density/A m ⁻²	Stirring speed/rpm
$\sqrt{2}$	46	341
+1	40	300
0	25	200
-1	10	100
$-\sqrt{2}$	4	58

3 Results and discussion

The low stability of baths 1 and 2 (Table 1) made it difficult to observe the reproducibility of the results and hindered their further use in the electrodeposition experiments. Similar results were obtained earlier [8, 12]. Therefore, the results presented here are related only to baths 3 and 4.

3.1 Polarization curves

Figure 1 shows the cathodic polarization curves of the steel electrode in solutions 3 and 4 (Table 1) for all S values used. The goals of these assays were to select the current density range for the electrodeposition tests and to verify the effects of both I and S on the cathodic performance of the electrolyte. The first part of these aims was wholly satisfied and the range between 1 and 50 $A\ m^{-2}$ was chosen (Table 3).

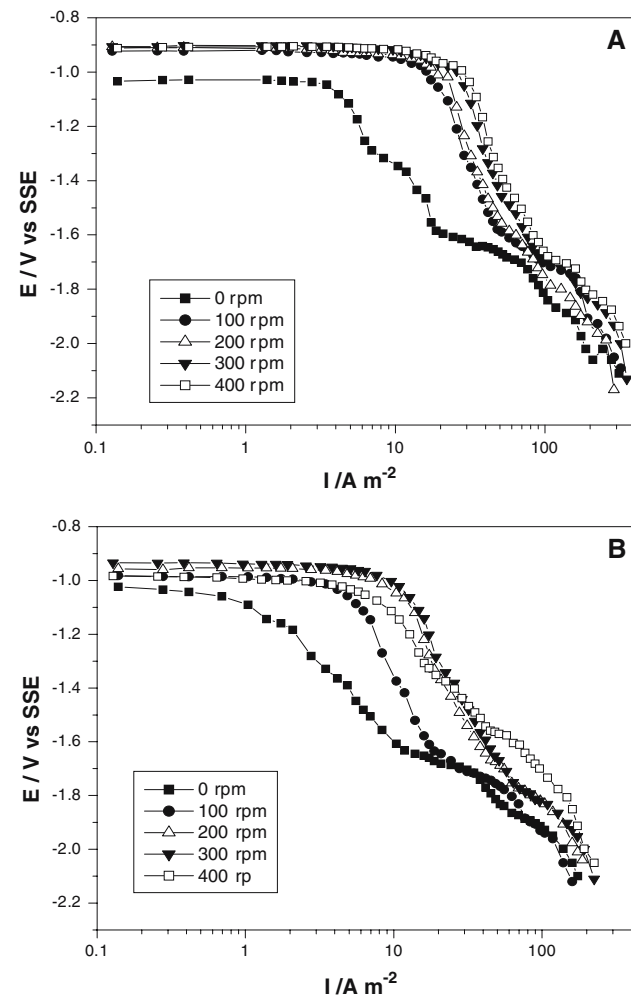


Fig. 1 Galvanostatic polarization curves in the solutions of Table 1: **(A)** Solution 3 and **(B)** Solution 4

For both solutions, the polarization curves have different slopes in different current density ranges, which is probably associated to several deposition mechanisms [16]. Additionally, the curves plotted at 0 rpm were more polarized than the others, especially for the current density range around 1 and 20 $A\ m^{-2}$. Increased S caused better ion transportation to the electrode surface. It is also important to note that the curves obtained in solution 4, with higher citrate amounts (Fig. 1b), were more polarized than those from solution 3 (Fig. 1a), irrespective of the S value used. Increasing the amount of citrate probably produces a joint effect of enhanced metal complexation and changed pH value to cause the observed polarization, as has been earlier verified for copper and zinc deposition in citrate medium [8, 10, 11]. Moreover, blocking species could also contribute to this polarization, making it difficult to deposit the metals.

3.2 Electrodeposition experiments

The effects of I and S can be better evaluated by applying experimental factorial procedures. Hydrogen evolution was also measured as I_H , obtained as the difference between the total current density and the (Cu+Zn) partial current densities (I_{Cu+Zn}). The values of I_{Cu+Zn} were calculated from the element contents in the alloy coating and the current efficiency [2, 3, 12].

The complete quadratic surface model between the response and the studied factors is given by Eq. (1).

$$\hat{y} = b_0 + b_1X_1 + b_2X_2 + b_{11}X_1^2 + b_{22}X_2^2 + b_{12}bX_1X_2 \tag{1}$$

where \hat{y} is the estimated response, X_1 corresponds to I , X_2 represents S , X_1X_2 is the interaction between I and S (IS), and b_i are the equation coefficients. Statistical tests ($p = 0.05$) were used to verify if the analyzed effects present any statistical significance. It is important to point out that even though some individual trends were observed in the responses based on the influence of I and S parameters, the final results were obtained by the complete quadratic response surfaces.

The results obtained for CCE are represented by Fig. 2, and by Eqs. (2) and (3) for baths 3 and 4, respectively. Each magnitude effect was presented only for conditions where significant influences were detected ($p < 0.05$). It is evident that, with a confidence level of 95%, neither I nor S had a significant effect ($p > 0.05$) on CCE for both baths. Therefore, a saddle point is observed in Fig. 2 for both solutions, indicating that high CCE values can probably be

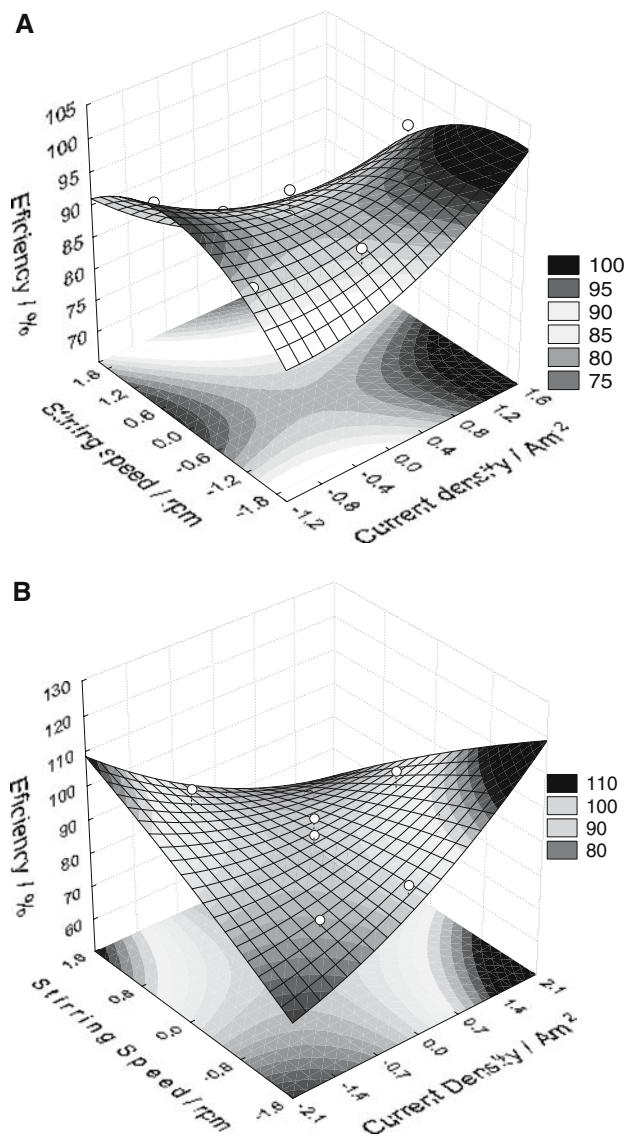


Fig. 2 Fitted surfaces of standardized effects for cathodic current efficiency (A) Bath 3; (B) Bath 4

obtained at high stirring speed and low current density, or at high current density and low stirring speed.

$$\hat{E} = 92 \quad (2)$$

$$\hat{E} = 88 \quad (3)$$

where \hat{E} represents *CCE*.

Similarly, it is possible to evaluate the effect of the studied factors on other electrodeposition parameters. Figure 3 presents the fitted surface responses for Cu content in the coatings produced from both solutions, while Eqs. (4) and (5) represent their models. For bath 3, where the copper-to-citrate concentration ratio was 1:25,

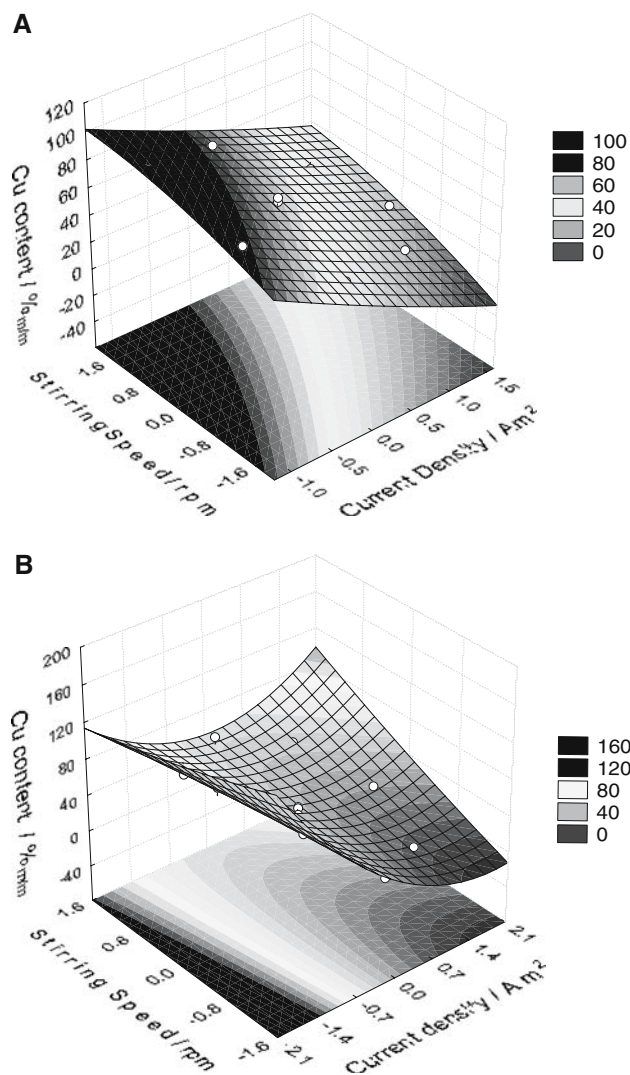


Fig. 3 Fitted surfaces of standardized effects for %m/m Cu (A) Bath 3; (B) Bath 4

both factors significantly influence the Cu content ($p < 0.001$ and $p < 0.02$, respectively). This influence is linear and negative for I , while linear and positive for S , as shown in Eq. (4) and Fig. 3a. Since Cu is a noble metal its ions are usually easily reduced and this is probably the main reaction observed at low values of current density. However, increasing I causes other parallel reduction reactions, such as Zn or H ion reduction, decreasing the amount of copper in the coating.

It is widely known that metallic ion transportation is favored by S , thus increasing the Cu content in the coating. Additionally, the proposed mechanisms for Cu deposition in citrate medium [8, 10], taking into account pH variation and citrate concentration, established that several Cu–citrate complexes are directly reduced without previous dissociation. After reduction, the resulting

species can be either directly incorporated into the deposit or undergo decomplexation, yielding molecules of free complexing agent. Therefore, an increase in S can enhance the transportation of any free ligand from the electrode surface to the solution bulk after discharge.

$$\hat{\%Cu} = 53 - 31I + 36S \tag{4}$$

In bath 4 (rate Cu:Citrate = 1:50), although the negative and linear influence of I is still apparent ($p < 0.00009$), there is no significant influence of S . Instead, there is a significant quadratic effect of I on the evaluated parameter ($p < 0.02$), as shown in Eq. (5) and Fig. 3b. Chassaing et al. [8] have shown that the direct inclusion of the copper-reduced complexes is proportional to the current density and to the surface concentration of the species to be included. In the present case, an increase in the amount of citrate in the bath would probably enhance the direct incorporation of the Cu–citrate complex species, mainly at high values of current density. Although the final response in Fig. 3b shows a quadratic influence, the linear effect seems to influence predominantly the copper content in the coating, which is in agreement with the p values.

$$\hat{\%Cu} = 36 - 23I + 13I^2 \tag{5}$$

Figure 4 shows the fitted surface responses for zinc content in the coating, while Eqs. (6) and (7) describe the resulting response of the model for both solutions. The studied factors affected the zinc reduction similarly, irrespective of the composition used. A direct influence of I on the Zn content ($p < 0.001$ and $p < 0.0002$ for baths 3 and 4, respectively) is noted, since large current densities are needed to promote the reduction of zinc ions to metallic zinc. On the other hand, a linear and negative influence of S on Zn content is also observed ($p < 0.004$ and $p < 0.003$ for baths 3 and 4, respectively). As seen earlier, forced convection may improve copper deposition, decreasing the zinc content in the coating. The fitted surfaces shown in Fig. 5 correspond to the model for zinc deposition using the studied citrate baths.

$$\hat{\%Zn} = 40 + 31I - 6.3S \tag{6}$$

$$\hat{\%Zn} = 54 + 28I - 4.0S \tag{7}$$

Therefore, based on Fig. 4, only coatings produced with high I and low S values had high zinc content. Moreover, some of these coatings, mainly at high

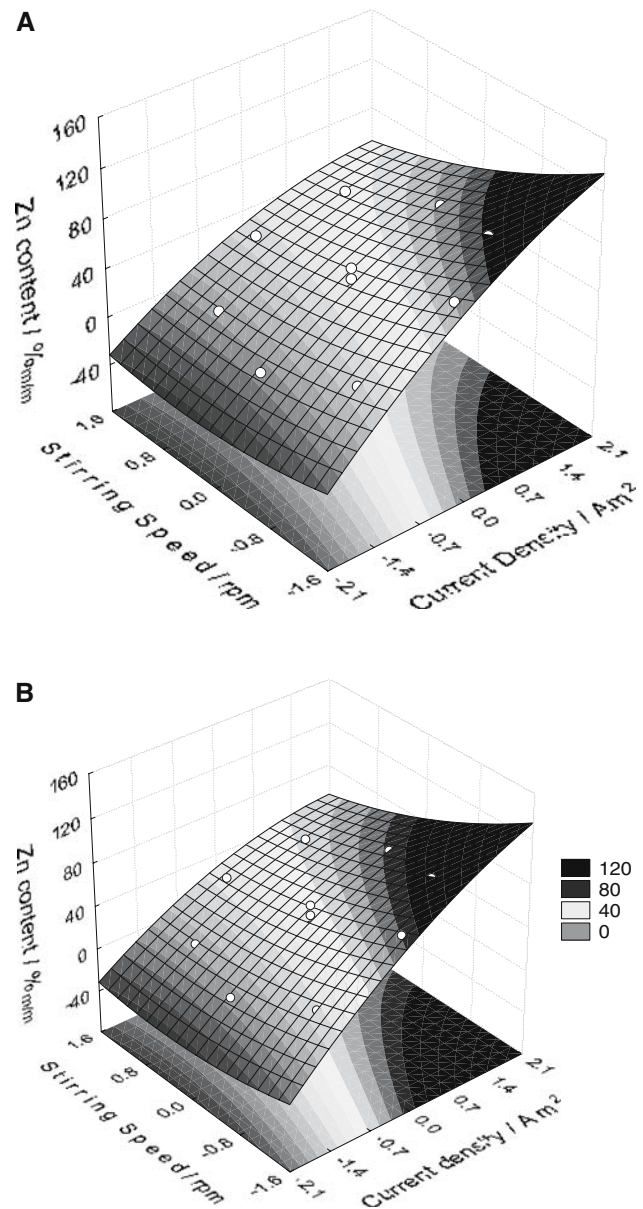


Fig. 4 Fitted surfaces of standardized effects for %m/m Zn (A) Bath 3; (B) Bath 4

current densities, presented a grayish color and low adhesion. Similar results were observed by Ishikawa et al. [17] and Senna et al. [3], who used pyrophosphate baths in alkaline solutions for deposition of Ni–Zn and Cu–Zn alloys, respectively, relating this behavior to hydrogen evolution and a consequent increase in pH near the electrode surface. In solutions containing only Zn–citrate complexes in the pH range 6.0–7.0, Gusev et al. [11] also suggested that the cathode could become passivated by hydroxides produced when the complexes decompose. As these complexes undergo discharge, the layer adjacent to

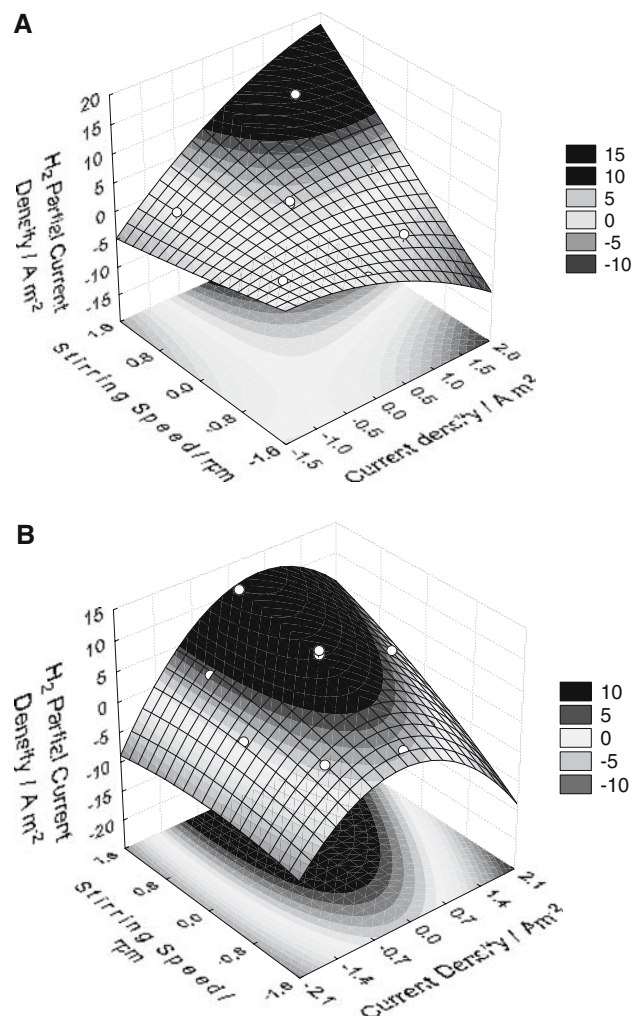


Fig. 5 Fitted surfaces of standardized effects for partial hydrogen current density (**A**) Bath 3; (**B**) Bath 4

the electrode becomes alkaline because of hydrolysis of the released citrate ions according to the reaction $C_6H_4O_7^{4-} + H_2O \rightleftharpoons C_6H_4O_7^{3-} + OH^-$, which also contributes to the appearance of hydroxyl ions in the near-surface layer. This phenomenon is favored by low S values, since the removal of $Zn(OH)_2$ precipitate occurs at a lower rate than its production in the layer next to the electrode.

It is also interesting to investigate the responses for I_H , since hydrogen reduction competes directly with the zinc reduction. The fitted surface responses (Fig. 5a and b) show that I and S affect this variable differently, depending on the bath used. In bath 3 (Eq. (8)), there is a direct and significant influence of S on I_H ($p < 0.02$). Additionally, a joint effect of I and S can be observed ($p < 0.04$). Analyzing these responses and the fitted response surface (Fig. 5a), hydrogen evolution is seen to occur preferentially at high current

densities and at high stirring speeds. At these conditions there is a huge competition between the reduction process of both zinc and hydrogen ions, since copper ion reduction is stimulated at high values of stirring speed but not at high current density. Therefore, the association of both studied effects would lead to the removal of zinc hydroxide from the electrode surface, decreasing the zinc content in the alloy. Although I_H is a calculated variable, depending on I_{Cu+Zn} [2, 3, 12], these conditions probably favor hydrogen reduction.

$$\hat{H} = 4.3 + 3.1S + 4.0IS \quad (8)$$

On the other hand, there is a significant and negative quadratic influence of I ($p < 0.04$) and a significant and positive effect of S ($p < 0.02$) on I_H obtained from bath 4 (Eq. (9)). The enhancement of I_H with S might again be explained by the removal of zinc hydroxide from the surface/solution interface, decreasing the zinc content and increasing I_H . Oppositely, an increase in I_H was expected with high I values, since under these conditions the formation of H_2 (g) is a parallel and competitive reaction to zinc ion reduction. However, by observing the corresponding fitted response surface (Fig. 5b) and Eq.(9), it is clear that the influence of current density on I_H cannot be analyzed alone as a negative quadratic effect. In fact, the joint effect of both parameters must be evaluated as a whole response, in which there is a trend toward increasing hydrogen evolution with stirring speed for a range of current densities. This is also in agreement with the p values for both variables.

$$\hat{H} = 7.7 - 3.0I^2 + 2.9S \quad (9)$$

Moreover, it is important to point out that these responses may not be completely independent and must be used with great care to characterize the trends in the hydrogen reduction process, since the I_H response was calculated from experimental results.

3.3 Optimization using the desirability function

Many response surfaces imply the analysis of several responses. Simultaneous consideration of multiple responses involves first building an appropriate response surface model for each response and then trying to find a set of operating conditions that, in some sense, optimizes all responses or, at least, keeps them in desired ranges. A useful approach to optimization of multiple responses is to use the simultaneous

optimization technique popularized by Derringer and Suich [15]. Their procedure makes use of desirability functions. The general approach is to first convert each response y_i , into an individual desirability function d_i that varies over the range $0 \leq d_i \leq 1$ where if response y_i is at its goal or target, then $d_i = 1$, and if the response is outside an acceptable region, $d_i = 0$. Next, the design variables are chosen to maximize the overall desirability, $D = (d_1 \cdot d_2 \cdot \dots \cdot d_m)^{1/m}$ where there are m responses.

The desirability function was used to evaluate all the responses found in the electrodeposition experiments for both solutions 3 and 4, in order to find an optimum point where the desired conditions (*CCE* values higher than 80%, Cu/Zn content ratio near the commercial brass values, and low I_H) could be obtained. Figure 6 presents the respective optimization surfaces.

The values of desirability obtained for both baths were smaller than 1 (0.53 and 0.36 for baths 3 and 4, respectively), showing that the estimated function might not completely represent the experimental model and the desired conditions, especially for bath 4. Keeping this in mind, coatings from both solutions were obtained at their respective optimized points and evaluated for their *CCE* values and Cu and Zn contents in the coating. Table 4 presents the optimized conditions and the attained results for the coatings produced in each bath. Since the desirability value for bath 4 was too small, the coating had a low *CCE* value and low Zn content, even though a bright red coating was obtained. Conversely, the *CCE* was over 80% in the coating from bath 3 and the Cu and Zn contents were near the commercial brass amounts. The coating had a bright yellow-reddish color.

3.4 Corrosion experiments

An optimized coating from bath 3 was again produced and submitted to corrosion experiments in 0.5 mol L⁻¹ NaCl solution. Figure 7 shows the results for the Cu–Zn layers produced in this bath and compares their electrochemical behavior with samples of copper, zinc and commercial brass. The coating showed a performance between that of pure copper and pure zinc, as expected for brass. Although its behavior was very different from that of commercial brass, it showed a superior protective behavior when compared to Cu–Zn coatings produced from a pyrophosphate bath without surfactants [3]. It is known that most of the electrolytically-obtained alloys produced from different baths usually consist of fine crystals, non-uniform in composition and characterized by a considerable distortion of the crystal lattice, originated during the formation of

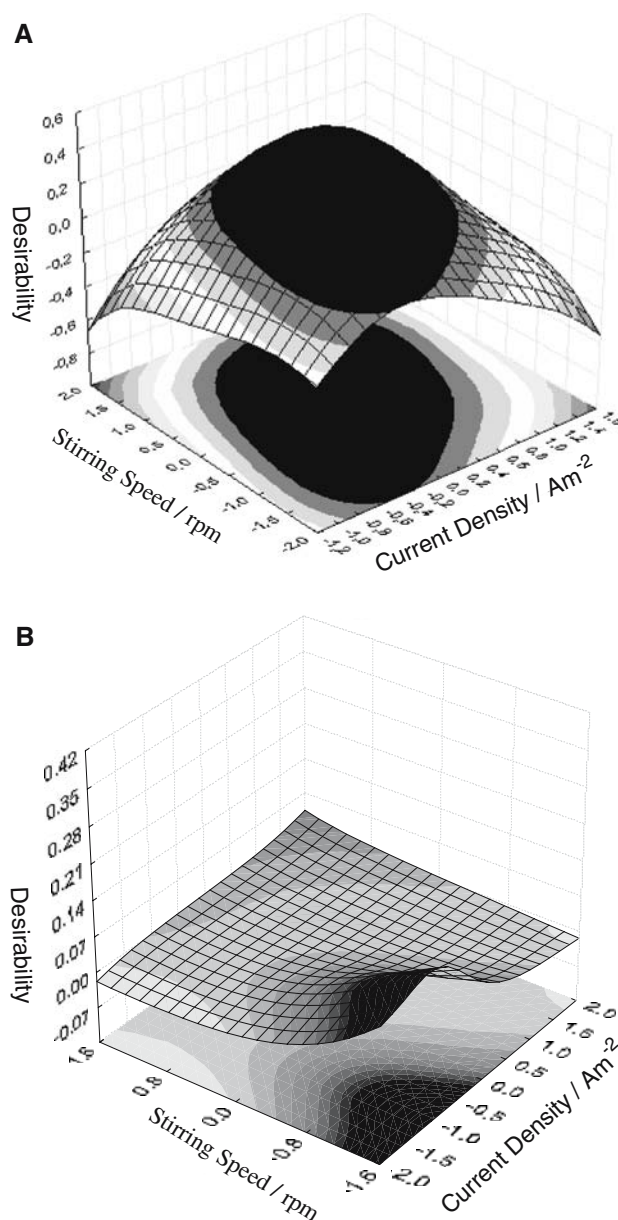


Fig. 6 Desirability fitted surfaces for baths 3 (A) and 4 (B)

Table 4 Optimized conditions and results of the experiments performed for both baths, at their respective optimum points (29 A m⁻² and 247 rpm, and 13 A m⁻² and 67 rpm for baths 3 and 4, respectively) based on the desirability function

Responses	Bath 3	Bath 4
Cathodic efficiency/%	85.0	23.0
Cu content/% m/m	80.5	82.0
Zn content/% m/m	20.5	0.2

the non-equilibrium phases at the cathode [1]. Lattice distortion may be responsible for non-homogeneous microscopic residual stress and can contribute

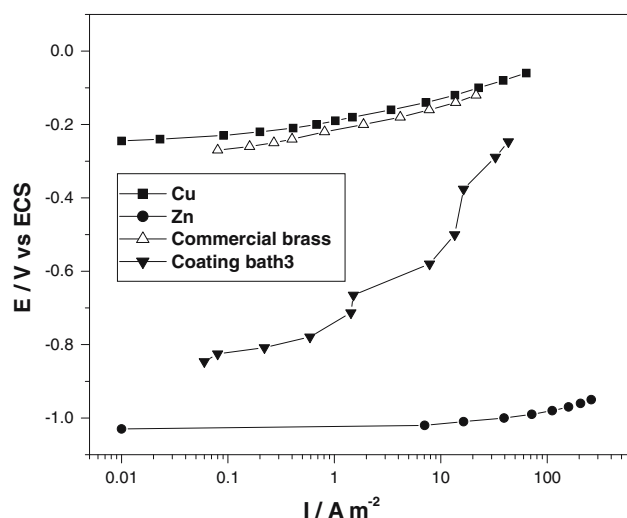


Fig. 7 Anodic polarization curves of coatings produced in bath 3 at its optimum point, based on the desirability function. Electrolyte: 0.5 mol L^{-1} NaCl, pH 6.5, 25°C

significantly to the coating microhardness [18, 19]. Therefore, although a very adherent coating was produced there were probably microdefects on the surface causing galvanic corrosion of the substrate, which explains the different behavior observed for the coating and the commercial brass. After the corrosion experiments the substrate/coating system showed localized corrosion.

4 Conclusion

Citrate baths containing sodium citrate concentrations equal to or higher than 0.5 mol L^{-1} can be used for electrodeposition of Cu–Zn alloy, producing shiny coatings whose colors vary from red to yellow-reddish. Gray coatings were also produced at high current density experiments.

The citrate concentration in the bath affected the electrodeposition process and, consequently, the content of the metals in the alloy coating. A higher polarization was noted due to the increase of citrate concentration in the bath, irrespective of the S value used. This could be a result of the increasing pH, the enhancement of metal–citrate complexes and the presence of blocking species on the electrode surface.

The deposition parameters (I and S) influenced Cu and Zn contents in opposite ways, mainly for coatings produced in bath 3. Increasing S favors the copper ion transport to the electrode surface, decreasing the zinc content in the coating. On the other hand, large I values enhance the zinc deposition and diminish the copper

quantity in the coating. There was also a quadratic and significant influence of the current density on the copper content in the coating for bath 4, which could be related to an increase in the direct incorporation of the reduced complexes with the current density.

The analysis of variance (ANOVA) shows that more than 85% and more than 90% of the results can be explained for Cu and Zn contents in the coating, respectively, irrespective of the bath composition used. The combined effect of the factors studied on copper and zinc contents resulted in a non-significant influence of these factors on the CCE . At high I values, I_H increased, mainly at high S values.

Optimized conditions for producing good quality Cu–Zn alloy coating (29 A m^{-2} and 247 rpm) were obtained by applying the desirability methodology, mainly for bath 3. The coating produced in this condition had high CCE values and Cu–Zn contents near to commercial brass. Its anticorrosion behavior was between pure Zn and pure Cu, showing localized corrosion after the electrochemical experiments. Conversely, the coating from bath 4 had a low CCE value and Zn content.

Acknowledgments The authors thank FAPERJ and UERJ for financial support.

References

- Vagramyan TA (1970) Electrodeposition of alloys: mechanism of simultaneous reaction of metal ions, Israel Program of Scientific Translation Ltd., Jerusalem
- Lainer VI (1970) Modern electrochemistry, Israel Program of Scientific Translation Ltd., Jerusalem
- Senna LF, Díaz SL, Sathler L (2003) *J Appl Electrochem* 33:1155
- Vagramyan TA, Solov'eva ZA (1961) Technology of electrodeposition. Robert Drapper Ltd., Teddington
- Fujiwara Y, Enomoto H (2000) *J Electrochem Soc* 147(5):1840
- Page D, Roy S (1997) *J Phy IV* 7(C5):269
- Krishnan RM, Muralidharan VS, Natarajan SR (1996) *Bull Electrochem* 12(5–6):274
- Chassaing E, Vu Quang K, Wiart R (1986) *J Appl Electrochem* 16:591
- Uksene V, Survila A, Žukauskaitė A (1996) *Rus J Electrochem* 32 (8):960
- Rode S, Heninot C, Vallières C, Matlosz M (2004) *J Electrochem Soc* 151(6):C405
- Gusev VN, Bezzubov AL, Kochman ED (1977) *Sov Electrochem* 13:111
- Assaf FA, Elrehim SSA, Mohamed AS, Zaky AM (1995) *Indian J Chem Technol* 2(3):147
- Senna LF (1991) Study of parameters for electroplating copper/zinc alloys from pyrophosphate electrolytes, M.Sc. thesis, Universidade Federal do Rio de Janeiro

14. Neto BB, Scarminio IS, Bruns RE (2001) Como Fazer Experimentos, Editora da UNICAMP, Campinas
15. Derringer G, Suich R (1980) J Qual Technol 12:214
16. Greef R, Peat R, Peter LM, Pletcher D, Robinson J (1985) Instrumental methods in electrochemistry, Ellis Horwood Limited, London
17. Ishikawa M, Enomoto H, Matsuoka M, Iwakura C (1994) Electrochim Acta 39(14):2153
18. Senna LF, Achete CA, Hirsch T, Mattos OR (2005) Surf Eng 21(2):144
19. Senna LF, Díaz SL, Sathler L (2005) Mat Res 8(3):275